JPET Fast Forward. Published on June 24, 2019 as DOI: 10.1124/jpet.119.259150
This article has not been copyedited and formatted. The final version may differ from this version.

Title Page

Title

Antiretroviral drug concentrations in lymph nodes: a cross-species comparison of the effect of drug transporter expression, viral infection, and sex in humanized mice, nonhuman primates, and humans[§]

Authors

Erin Burgunder, John K. Fallon, Nicole White, Amanda P. Schauer, Craig Sykes, Leila Remling-Mulder, Martina Kovarova, Lourdes Adamson, Paul Luciw, J. Victor Garcia, Ramesh Akkina, Philip C. Smith, and Angela DM Kashuba

Primary Laboratory of Origin

Angela DM Kashuba, Clinical Pharmacology and Analytical Chemistry Laboratory, 1094 Genetic Medicine Building CB#7361, 120 Mason Farm Road, University of North Carolina at Chapel Hill, Chapel Hill, North Carolina, 27599 United States

Affiliation

EB, JKF, NW, AS, CS, PCS, ADMK; Eshelman School of Pharmacy, University of North Carolina at Chapel Hill, Chapel Hill, North Carolina, United States

LR-M, RA; School of Medicine, Colorado State University, Fort Collins, Colorado, United States

LA, PL; School of Medicine, University of California Davis, Davis, California, United States

MK, JVG, ADMK; School of Medicine, University of North Carolina at Chapel Hill, Chapel Hill, North Carolina, United States

Running Title Page

a) Running Title

Factors affecting lymph node ARV penetration in three species

b) Corresponding Author

Dr. Angela DM Kashuba, BScPhm, PharmD, DABCP

1094 Genetic Medicine Building, CB#7361

120 Mason Farm Road

Eshelman School of Pharmacy, Division of Pharmacotherapy and Experimental Therapeutics

University of North Carolina at Chapel Hill

Chapel Hill, North Carolina 27599-7569

Phone: (919) 996-9998

Fax: (919) 966-1020

akashuba@unc.edu

c) Number of text pages:

Number of tables: 1

Number of figures: 6

Number of references: 58

Number of words in *Abstract*: 247/250

Number of words in *Introduction*: 475/750

Number of words in *Discussion*: 1498/1500

d) Abbreviations

ANOVA—analysis of variance

ART—antiretroviral therapy

ARV—antiretroviral

ATZ—atazanavir

AUC—area under the curve

BCRP—breast cancer resistance protein

BLD—below the limit of detection

BLQ—below the limit of quantification

BLT—bone marrow-liver-thymus humanized mice

dATP—deoxyadenosine triphosphate

dCTP—deoxycytidine triphosphate

EC_{90}—90% effective concentration

EFV—efavirenz

ENT1—equilibrative nucleoside transporter 1

FTC—emtricitabine

FTCtp—emtricitabine triphosphate

GAPDH—glyceraldehyde 3-phosphate dehydrogenase

HPLC—high performance liquid chromatography

IACUC— Institutional Animal Care and Use Committee

IHC—immunohistochemistry

LC-MS/MS—liquid chromatography mass spectrometry/mass spectrometry

LLOD—lower limit of detection

LLOQ—lower limit of quantitation

LNMC—lymph node mononuclear cells

MRM—multiple reaction monitoring

MRP1—multidrug resistance-associated protein 1

MRP2—multidrug resistance-associated protein 2

MRP4—multidrug resistance-associated protein 4

MSI—mass spectrometry imaging

MVC—maraviroc

NDRI—National Disease Research Interchange

NHP—nonhuman primate

NNTC—National NeuroAIDS Tissue Consortium

OATP2A1—organic anion transporting polypeptide 2A1

OCT3—organic cation transporter 3

PBMC—peripheral blood mononuclear cells

PK/PD—pharmacokinetic/pharmacodynamic

PGP—P-glycoprotein

qPCR—quantitative polymerase chain reaction

QTAP—quantitative targeted absolute proteomics

RagHu—hu-HSC-Rag humanized mice

RAL—raltegravir

RT-SHIV—reverse transcriptase-simian/human immunodeficiency virus

SIL—stable isotope labeled

TFV—tenofovir

TFVdp—tenofovir diphosphate

TPR—tissue penetration ratio

e) Recommended section assignment

Metabolism, Transport, and Pharmacogenomics

JPET Fast Forward. Published on June 24, 2019 as DOI: 10.1124/jpet.119.259150
This article has not been copyedited and formatted. The final version may differ from this version.

Abstract

In a “kick and kill” strategy for HIV eradication, protective concentrations of antiretrovirals (ARVs) in the lymph node are important to prevent vulnerable cells from further HIV infection. However, the factors responsible for drug distribution and concentration into these tissues are largely unknown. While humanized mice and nonhuman primates (NHPs) are crucial to HIV research, ARV tissue pharmacology has not been well characterized across species. This study investigated the influence of drug transporter expression, viral infection, and sex on ARV penetration within lymph nodes of animal models and humans. Six ARVs were dosed for 10 days in humanized mice and NHPs. At necropsy, 24h after the last dose, plasma and lymph nodes were collected. Human lymph node tissue and plasma from deceased patients were collected from tissue banks. ARV, active metabolite, and endogenous nucleotide concentrations were measured by LC-MS/MS, and drug transporter expression was measured using qPCR and quantitative targeted absolute proteomics (QTAP). In NHPs and humans, lymph node ARV concentrations were greater than or equal to plasma, and TFVdp:dATP concentration ratios achieved efficacy targets in lymph nodes from all 3 species. There was no effect of infection or sex on ARV concentrations. Low drug transporter expression existed in lymph nodes from all species, and no predictive relationships were found between transporter gene/protein expression and ARV penetration. Overall, common preclinical models of HIV infection were well suited to predict human ARV exposure in lymph nodes, and low transporter expression suggests primarily passive drug distribution in these tissues.

JPET Fast Forward. Published on June 24, 2019 as DOI: 10.1124/jpet.119.259150
This article has not been copyedited and formatted. The final version may differ from this version.

Significance Statement

During HIV eradication strategies, protective concentrations of antiretrovirals (ARVs) in the lymph node prevent vulnerable cells from further HIV infection. However, ARV tissue pharmacology has not been well characterized across preclinical species used for HIV eradication research, and the influence of drug transporters, HIV infection, and sex on ARV distribution and concentration into the lymph node is largely unknown. Here we show that two animal models of HIV infection (humanized mice and nonhuman primates) were well suited to predict human ARV exposure in lymph nodes. Additionally, we found that drug transporter expression was minimal, and—along with viral infection and sex—did not affect ARV penetration into lymph nodes from any species.

Introduction

Advances in antiretroviral therapy (ART) potency and dosing have transformed HIV from a fatal diagnosis to a chronic condition, with patient life expectancy now comparable to that of an uninfected population (Samji *et al.*, 2013). Despite this, challenges in treating and curing HIV remain (Lewin and Rouzioux, 2011). While the majority of patients adherent to ART show undetectable viral replication in blood plasma, viral rebound occurs upon interruption of therapy (Chun *et al.*, 1999). One theoretical cause of viral rebound is low-level viral replication within tissues (Natarajan *et al.*, 1999; Buzón *et al.*, 2011), caused by inadequate antiretroviral (ARV) penetration (Horiike *et al.*, 2012; Fletcher *et al.*, 2014; Fletcher, 2018). Low ARV penetration may also present challenges in protecting cells from infection during “kick and kill” strategies for HIV eradication (Lewin and Rouzioux, 2011).

In the area of HIV prevention, investigations into drug concentrations in colorectal and female genital tract tissues have shown highly variable ARV penetration (Dumond *et al.*, 2007, 2009; Kwara *et al.*, 2008; Else *et al.*, 2011; Patterson *et al.*, 2011; Thompson *et al.*, 2015; Cottrell *et al.*, 2016). However, considerably less drug exposure data are available for the putative lymph node reservoir, despite the fact that these tissues are central to the pathology of HIV (North *et al.*, 2010; Dimopoulos *et al.*, 2017). In the small number of published studies, results are conflicting. ARV lymph node concentrations range from 2-fold higher to 1000-fold lower than those in plasma (Kinman *et al.*, 2003; Solas *et al.*, 2003; Fletcher *et al.*, 2014). Furthermore, the methods used to investigate drug penetration in lymph nodes are also varied; some studies have used tissue homogenate (Solas *et al.*, 2003), while others have isolated lymph node mononuclear cells (LNMCs) (Kinman *et al.*, 2003; Fletcher *et al.*, 2014).

Because human lymph node collection is invasive, pre-clinical models such as HIV-infected humanized mice and nonhuman primates (NHPs) with reverse transcriptase-simian/human immunodeficiency virus (RT-SHIV) may be informative for characterizing the pharmacokinetics of ARVs in lymph nodes. Pre-clinical models have been used to assess viral

dynamics in tissues and curative ART strategies, (Denton and García, 2011; Evans and Silvestri, 2013), but a cross-species comparison of ARV concentrations in putative tissue reservoirs is still needed. Furthermore, in order to understand concentration-response relationships of ARVs in tissues, it is important to investigate relevant biological and disease-related factors that may influence these concentrations, such as drug transporters, viral infection, and sex (Antonelli *et al.*, 1992; Speck *et al.*, 2002; Fletcher *et al.*, 2004; Giraud *et al.*, 2010; Alam *et al.*, 2016; Kis *et al.*, 2016).

In this study, we aimed to quantify ARV concentrations and these aforementioned influencing factors using lymph nodes from humanized mice, NHPs, and deceased HIV+ patients. We believe that these data improve our understanding of ARV pharmacology in the lymph node—an important but pharmacologically less characterized HIV tissue reservoir.

Materials and Methods

Animal Studies and Lymph Node Collection

A detailed description of the animal studies is has been published previously (Thompson *et al.*, 2017), and is summarized here. This study used 3 common HIV preclinical models from 2 species: hu-HSC-Rag (RagHu) humanized mice (n=36), bone marrow-liver-thymus (BLT) humanized mice (n=13), and rhesus macaques (NHP) (n=18). All humanized mice and 6 NHPs were female. Aggressive interactions are common between male mice within the same cage, but isolating mice in separate cages can be inefficient and costly. For these reasons, we chose to use only female mice that could be safely kept in groups to minimize cage needs while maximizing animal well-being (Van Loo *et al.*, 2003). RagHu mice (n=18), BLT mice (n=7), and NHPs (n=10) were infected for 6 weeks with $HIV_{BAL\ D7}$, HIV_{JRcsf}, and RT-SHIV, respectively (North *et al.*, 2010). The remaining animals were uninfected (RagHu n=18, BLT n=6, NHP n=8). After the infection period, animals were dosed for 10 days to steady-state and necropsy was performed one day after the last dose. Doses were chosen based on previously reported effective treatment regimens in these animal models (Denton *et al.*, 2010; Neff *et al.*, 2010; Shytaj *et al.*, 2012; Massud *et al.*, 2013; Veselinovic *et al.*, 2014), and are reported in Supplemental Data. RagHu mice were dosed with efavirenz (EFV) only (n=12), atazanavir (ATZ) only (n=12) or a combination of tenofovir (TFV), emtricitabine (FTC), raltegravir (RAL), and maraviroc (MVC) (n=12). All BLT mice received the 5 drug combination of TFV/FTC/RAL/MVC/ATZ (n=13). Finally, NHPs were dosed with TFV/FTC/EFV/RAL (n=9) or TFV/FTC/MVC/ATZ (n=9). Further details on animal dosing, infection, and tissue collection can be found in Supplemental Data, Supplemental Figure 1, and Supplemental Table 1.

At necropsy, plasma and lymph nodes were collected from all animals and snap frozen. For both RagHu and BLT mice, lymph node type was not determined, while in NHPs, 4 lymph nodes (mesenteric, axillary, inguinal, and iliac) per animal were collected. Mouse and NHP tissue was divided for use in ARV and transporter expression analyses, with matched data obtained

when possible (Supplemental Table 2). All animal studies were performed in accordance with Institutional Animal Care and Use Committee (IACUC) protocols from the University of North Carolina at Chapel Hill (protocol 15-168), Colorado State university (protocol 16-6998A), and the University of California Davis (protocol 18345).

Human Lymph Node Collection

Human plasma and lymph node samples were obtained by the National Research Disease Interchange (NDRI) and the National NeuroAIDS Tissue Consortium (NNTC) from deceased HIV+ patients who consented to organ donation prior to death, or whose families consented to organ donation immediately following the patients' death. To screen for subjects who were adherent to ART or received ARV dosing pre-mortem (and therefore most likely to have quantifiable tissue ARV concentrations), plasma samples were obtained based on desired subject characteristics such as tissue availability, viral load, and ART regimens containing TFV, FTC, EFV, RAL, MVC, or ATZ. Plasma samples were analyzed in our laboratory by LC-MS/MS, and only subjects with measurable ARV plasma concentrations were included in the tissue request. Ultimately, lymph node sections from 13 subjects (2 female) were requested, and each subject's ART regimen contained at least one drug of interest (8 TFV, 4 FTC, 7 EFV, 3 RAL, 2 ATZ, 0 MVC). Human lymph node tissue was divided for use in ARV and transporter expression analyses, with matched data obtained when possible (Supplemental Table 2). Details on subject demographics, virology, ART dosing/regimens and preliminary plasma ARV concentrations can be found in Supplemental Table 3.

ARV Concentration and Tissue Penetration Analyses

Concentrations of all 6 ARVs (TFV, FTC, EFV, RAL, MVC, and ATZ) were analyzed in plasma and lymph node tissue using LC-MS/MS. Additionally, the intracellular active metabolites tenofovir diphosphate (TFVdp) and emtricitabine triphosphate (FTCtp), and their respective endogenous nucleotides, deoxyadenosine triphosphate (dATP) and deoxycytidine triphosphate (dCTP), were analyzed in lymph node tissue.

Plasma and tissue samples were extracted by protein precipitation using stable, isotopically labeled internal standards. Extracts were analyzed by a Shimadzu HPLC system with an API 5000 mass spectrometer (SCIEX, Framingham, MA) detector equipped with a TurboIonSpray interface. The lower limit of quantitation (LLOQ) for plasma was 1 ng/mL, and for tissue was 0.002 ng/mL (FTC, MVC), 0.005 ng/mL (EFV, RAL, ATZ), 0.01 ng/mL (TFV), 1.11 ng/mL (dATP, dCTP), and 0.22 ng/mL (TFVdp, FTCtp). Assay precision and accuracy was within 15%.

At least 30 mg of lymph node tissue was homogenized using a Precellys Tissue Homogenizer (Bertin Technologies, Montigny-le-Bretonneux, France) in 1 mL of 70:30 acetonitrile:1 mM ammonium phosphate (pH 7.4) and extracted by protein precipitation as before. TFV and FTC were analyzed using a Waters Atlantis T3 (50mm x 2.1mm, 3 µm particle size) column; EFV, RAL, MVC, and ATZ were separated using an Agilent Pursuit XRs 3 Diphenyl (50 mm x 2 mm, 5 µm particle size) HPLC column; TFVdp, FTCtp, dATP, and dCTP were analyzed on a Thermo BioBasic AX column. Concentrations were converted from ng/ml to ng/g based on a tissue density of 1.06 g/ml.

Tissue penetration ratios (TPRs) at the end of the dosing interval were calculated for each ARV by dividing lymph node concentrations by plasma concentrations. We also calculated active metabolite to endogenous nucleotide ratios, since the efficacy of the active metabolite depends on its concentration relative to the endogenous nucleotide it replaces during reverse transcription (Anderson *et al.*, 2011).

Protein Expression Analysis

Protein concentrations of 5 efflux and 3 uptake transporters were measured by quantitative targeted absolute proteomics (QTAP) (Fallon *et al.*, 2013). Transporters were chosen based on their relevance to ARV disposition, putative expression in lymph nodes, or previous investigation in other reservoir tissues (Supplemental Table 4) (Minuesa *et al.*, 2011; Zhou *et al.*, 2013; Nicol *et al.*, 2014; Huang *et al.*, 2016; Thompson *et al.*, 2017). Approximately 100 mg of

lymph node tissue was homogenized in 1.3 mL of hypotonic buffer (10 mM NaCl, 1.5mM $MgCl_2$, 10 mM Tris HCl pH 7.4, 150 µL Complete Protease Inhibitor Solution (Sigma Aldrich, St. Louis, MO)) using a Precellys Tissue Homogenizer, and 10-30 µg of membrane protein was isolated as previously described (Fallon *et al.*, 2016; Thompson *et al.*, 2017). Membrane protein was dried down and reconstituted with 50 mM ammonium bicarbonate buffer plus 40 mM dithiothreitol, 10% sodium deoxycholate, and 10 µL β-casein (0.1 µg/µL). Samples were then reduced for 40 min at 60 ºC followed by addition of 135 mM iodoacetamide and incubation in the dark for 30 min at room temperature. One pmol of stable isotope labeled (SIL) peptide standards (Theracode JPT Inc, Acton, MA) were added to samples, followed by digestion with 25 µL trypsin (0.1 µg/µL) at 37 ºC (Promega, Madison, WI). Digestion was interrupted after 18 h with 10% trifluoroacetic acid, and samples were extracted using solid phase extraction on 33 µm polymeric reversed phase extraction columns (Phenomonex, Torrance, CA). After final dry-down and reconstitution in 98% formic acid (0.1%) plus 2% acetonitrile, around 0.06-0.12 µg of microsomal protein was loaded onto a C18 trap column connected to a BEH130 C18 (150 µm x 100 mm, 1.7 µm particle size) main separation column. Sample analysis was performed on a nanoACQUITY system (Waters, Milford, MA) coupled to a Qtrap 5500 mass spectrometer (SCIEX, Framingham, MA) equipped with a Nanospray III source. Analyst 1.5 and MultiQuant 2.0 software (SCIEX) were used for multiple reaction monitoring (MRM) data acquisition and analysis. Peak area ratios of unlabeled/SIL peptides were determined using the sum of two MRMs. The lower limit of detection (LLOD) for the peptides was 0.1 pmol/mg protein, and 50 µg NHP liver homogenate was used as a positive control.

Gene Expression Analysis

Gene expression of the same 8 transporters was measured by qPCR. Approximately 30 mg of tissue was homogenized using a Precellys Tissue Homogenizer and RNA was extracted using a Qiagen RNAeasy Fibrous Tissue Mini Kit (Qiagen, Valencia, CA). The VILO Superscript cDNA Synthesis Kit (Thermo Fisher, Waltham, MA) was used to reverse transcribe 200 ng of

RNA. A 10-cycle pre-amplification was performed, followed by 40 cycles of qPCR using Taqman primers and probes (Supplementary Table 5) on a QuantStudio6 (Life Technologies, Waltham, MA). Samples were run in triplicate, and transporter expression was normalized to the housekeeping gene GAPDH using the $2^{-\Delta CT}$ method (Schmittgen and Livak, 2008). The LLOD was a 0.0001 fold change over GAPDH.

Statistical Analysis

In all species, ARV concentrations, gene expression values, or transporter protein concentrations below the limit of detection/quantitation (BLD/BLQ) of the assay were imputed at half the LLOQ or LLOD, respectively. Relationships between plasma and lymph node drug concentrations were assessed using linear regression. Comparisons between species, infection status, and sex were performed using the Kruskal-Wallis One-Way ANOVA test with Dunn's Method for multiple comparisons, and relationships between transporter expression and TPRs were investigated using multiple linear regression. Data were analyzed using SigmaPlot 13.0 (Systat Software Inc., San Jose, CA) with a significance level of $p<0.05$.

Results

There were no statistically significant differences in ARV concentrations between the 4 lymph nodes collected from each NHP (either uninfected or infected) (Supplemental Figure 2), so data from all lymph nodes were averaged to generate one median value for each uninfected or infected animal. Plasma and lymph node ARV concentrations were not significantly different between BLT and RagHu mice, so data from both humanized mouse species were pooled for the remaining analyses (Supplemental Figure 3). One female macaque dosed with TFV/FTC/EFVRAL developed liver failure, resulting in drug concentrations 17- to 260-fold higher than other animals in the dosing group. This NHP was excluded from ARV concentration/penetration analyses, but was included in drug transporter comparisons; transporter expression was not significantly different from other animals in the dosing group. Additionally, to avoid overestimating lymph node ARV penetration, mice and NHPs with BLQ plasma concentrations but measurable lymph node concentrations were excluded from analyses. These sample size adjustments are reflected in Supplemental Table 2.

ARV concentrations in plasma and lymph nodes:

Several species-dependent trends in ARV concentrations and lymph node penetration relative to plasma were noted. Median ARV plasma concentrations were generally lowest in mice (14% BLQ) and highest in humans, with a few exceptions: FTC and TFV were lowest in NHPs rather than mice, and RAL was highest in NHPs rather than humans; however, only one human plasma sample was available for RAL analysis (Figure 1A). In lymph nodes, median ARV concentrations followed the same species trends seen in plasma, with 46% of mouse concentrations BLQ. The only notable differences were in TFV (highest in NHPs rather than humans) and RAL (highest in humans) (Figure 1B). TPRs were calculated using matched lymph node and plasma concentrations. Median NHP lymph node TPRs ranged from 3-fold lower (RAL) to 25-fold higher (MVC) than plasma (Figure 2). Compared to other species, NHP TPRs were highest for all drugs except FTC and RAL. Median mouse TPRs ranged from 0.0002 (RAL) to 8

(FTC), and human TPRs from 0.8 (ATZ) to 2 (EFV). Excluding BLQ concentrations in mice, there were several significant relationships between lymph node and plasma concentrations: FTC (r^2 = 0.73, $p<0.001$), TFV (r^2 = 0.03), EFV (r^2 = 0.73, $p<0.001$), RAL (r^2 = 0.004), MVC (r^2 = 0.40, $p<0.05$), and ATZ (r^2 = 0.55, $p<0.01$).

Active metabolite and endogenous nucleotide concentrations and ratios:

Active metabolite concentrations showed greater between-species variability than parent drugs, particularly for TFVdp. Similar to the pattern of TFV TPRs, median TFVdp concentrations were highest in NHPs (Figure 3A). On a molar basis, lymph nodes from all species contained more parent drugs than active metabolites, but NHPs had the greatest proportion of FTC converted to FTCtp (4.8%; mouse = 0.2%, human = 1.1%) and TFV converted to TFVdp (6.4%; mouse = 0.1%, human = 0.2%) (Table 1). Concentrations of the endogenous nucleotides dCTP and dATP were highest in NHP lymph nodes, but not significantly different across species (Figure 3A). When comparing endogenous nucleotides to corresponding active metabolites, only NHP dATP concentrations were significantly different from TFVdp concentrations ($p<0.05$). Therefore, after normalizing active metabolite concentrations to endogenous nucleotides, TFVdp:dATP ratios were significantly higher in NHPs, but FTCtp:dCTP ratios were similar across species (Figure 3B).

Effect of viral infection and sex on ARV penetration in lymph nodes:

No differences in lymph node drug penetration due to viral infection (Figure 4) or sex (Figure 5) were found in any species. There were also no trends in the variability of ARV penetration between uninfected and infected animals, or males and females.

Drug transporter expression in lymph nodes:

Lymph node drug transporter expression was low across all species. Gene expression of all 8 transporters was consistently lower than the housekeeping gene GAPDH in both mice and NHPs (Figure 6A). Median ENT1 gene expression was highest overall for both species. Mouse gene expression was higher than NHP for all transporters but MRP2. Transporter protein

expression was also low in NHP and human lymph nodes; BCRP, ENT1, and OCT3 were the only NHP transporters with median concentrations above the limit of detection (94%, 100%, and 94% of samples above LLOD, respectively), and in humans median concentrations of all 8 transporters were below the limit of detection (Figure 6B).

Effect of drug transporter expression on ARV lymph node penetration:

Few predictive relationships were found between ARV TPRs and drug transporter expression. Higher mouse and NHP gene expression of MRP2 was predictive of greater TFV penetration in lymph nodes ($p=0.002$, $r^2 = 0.27$) (Supplementary Table 6), and greater ATZ penetration in NHPs and humans was predicted by an increase in combined MRP1 and PGP protein expression ($p<0.001$, $r^2 = 0.99$) (Supplementary Table 7).

Discussion

This study is the first to evaluate ARV exposure in lymph nodes of three species. In this investigation, we determined that there was no effect of acute HIV infection or sex on ARV lymph node concentrations. However, we did find several interesting species-dependent differences in drug exposure. In mice, EFV, RAL, MVC, and ATZ penetration was low and variable: between 33% (EFV) and 83% (RAL) of lymph node concentrations were BLQ. No relationship was found between the amount of mouse lymph node analyzed and tissue concentrations, indicating that BLQ concentrations are not the result of small tissue quantities and LC-MS/MS sensitivity. There were also no animal-specific trends in tissue concentrations: previous analyses found no BLQ concentrations in brain tissue from any mouse, while 96% of ileum and 87% of rectum concentrations were BLQ in the same animals (Thompson, 2017; Srinivas *et al.*, 2018). When considering only mice with quantifiable lymph node concentrations, drug penetration was generally similar between mice, NHPs, and humans.

Similar to the pattern of TFV penetration ratios, TFVdp concentrations and TFVdp:dATP ratios in were significantly higher in NHPs. Previous work in NHPs and humans has shown that in target lymphoid organs, the concentration ratio of TFVdp to the endogenous substrate dATP may be a better predictor of efficacy than TFVdp concentrations alone (García-Lerma *et al.*, 2011; Cottrell *et al.*, 2016). Using an in vitro enzymatic inhibition assay, investigators have shown that a TFVdp:dATP ratio ≥ 1 corresponds to 100% reverse transcriptase inhibition in NHPs (García-Lerma *et al.*, 2011). In our study, median NHP TFVdp:dATP ratios were 34, well above an efficacy target of one. Similarly, a predictive PK/PD model in humans found a 90% effective TFVdp:dATP concentration ratio (EC_{90}) of 0.29 for protecting CD4+ T cells from viral challenge (Cottrell *et al.*, 2016); in our study, this efficacy target was exceeded by NHPs and humans, and almost achieved in mice (median ratios of 34, 1, and 0.2, respectively). These data show that despite a species difference in TFVdp concentrations, both preclinical species meet previously-investigated human TFVdp:dATP efficacy targets in lymph node tissue.

A previous study reported that TFVdp concentrations in human LNMCs were significantly lower than in PBMCs, and that these low concentrations were associated with HIV replication (Fletcher *et al.*, 2014). Indeed, it is well known that even during suppressive ART, viral RNA and DNA can persist in lymph nodes and other tissues from NHPs and humans (North *et al.*, 2010; Deleage *et al.*, 2016; Lamers *et al.*, 2016; Estes *et al.*, 2017), and there may be evidence of ongoing HIV replication within the lymph nodes of ART–suppressed patients (Lorenzo-Redondo *et al.*, 2016; Halvas, 2019). However, in contrast to previous LNMC studies—which do not account for drug lost during cell isolation and may underestimate concentrations—we found that lymph node TFV concentrations are higher than or equal to plasma, and TFVdp:dATP ratios meet or exceed the EC_{90} target to inhibit HIV reverse transcription.

Yet the concentrations we have presented are an averaged concentration throughout the lymph node. It has been previously demonstrated that drug distribution within a tissue can be variable (Fischman *et al.*, 1998), and we have shown heterogeneous efavirenz concentrations across 5 different putative tissue reservoirs using mass spectrometry imaging (MSI) (Thompson *et al.*, 2015). Recently, we also saw little co-localization of viral RNA with efficacious ARV concentrations in brain (3% overlap) (Srinivas *et al.*, 2018). Therefore, an ARV's *location* within tissue is as important as overall concentration. We are continuing to evaluate lymph node distribution by quantitative MSI to address this issue.

In addition to ARV concentrations, this study was also the first to examine cross-species expression of relevant ARV transporters in lymph nodes. Overall, transporter expression in lymph nodes is comparable to what we have seen in brain tissue (Srinivas, 2018), but lower than other HIV reservoirs such as testis, ileum, and rectum (Huang *et al.*, 2016; Thompson *et al.*, 2017). The most highly expressed transporter by gene and protein methods was ENT1. This aligns with previous RNA expression and immunocytochemistry data for ENT1 in lymphoblastic T-cell lines and CD4+ T cells isolated from HIV- donors (Minuesa *et al.*, 2008). ENT1 is responsible for the cellular uptake of nucleosides such as adenosine and uridine, which are important for

immunostimulatory responses and lymphocyte proliferation (Goodman and Weigle, 1983, 1984); therefore, increased ENT1 expression in lymph nodes is not unexpected.

To determine if even low-level transporter expression could influence drug distribution in the lymph node, we used multilinear regression to assess relationships between ARV penetration ratios and transporter gene/protein expression across species, including any potential link between ENT1 expression and TFV—an adenosine analog (Gilead Sciences, Inc., 2001). While the positive associations between TFV vs. MRP2 (in mice and NHPs) and ATZ vs. MRP1+PGP (in NHPs and humans) are significant, these relationships were primarily driven by the number of BLD transporter concentrations, and are inconsistent with the intracellular-to-extracellular direction of MRP1, MRP2, and PGP efflux transporters. Taken together, generally low drug transporter expression in the lymph node, and lack of physiologically-relevant predictive relationships between transporters and ARV penetration, suggests that drug distribution in the lymph node may occur by passive, diffusion-based mechanisms—contributing to the heterogeneous ARV distribution we have seen in the lymph node for efavirenz (Thompson *et al.*, 2015).

There are several limitations in our assessment of ARV tissue penetration. One important consideration is our use of steady-state plasma and tissue concentrations obtained at the end of the dosing interval to estimate tissue penetration ratios. This approach may overestimate drug penetration into lymph nodes, since the difference in drug concentrations in these two compartments is likely greatest at the end of the dosing interval. A better method of estimating tissue penetration is by dividing lymph node and plasma areas under the concentration time curves ($AUC_{tissue}/AUC_{plasma}$), which can be determined by repeated tissue sampling. However, in our animal studies, we opted to start collecting a set of whole lymph nodes at the end of the dosing interval. A second possible limitation is blood contamination within lymph node homogenate, although no blood was observed during visual inspection of the tissue. Using MSI we have analyzed lymph node sections for heme—a blood marker—and ARVs, and have found little co-

localization of the two (≤25% overlap) (unpublished). We will continue these analyses in the future to correct for blood contamination in the lymph node. Finally, lymph node ARV concentrations reported here include both protein bound and unbound fractions. Preliminary studies in a small set of NHP samples suggest that RAL, MVC, and ATZ binding is minimal in lymph nodes (<50% bound), while EFV binding is comparable to plasma (≈97% bound) (unpublished). Further binding analyses are ongoing.

Additionally, there were several limitations to our drug transporter analyses. We were unable to compare all tissues for gene and protein expression. Although protein expression is a more relevant measure of transporter presence in tissue (Ohtsuki *et al.*, 2012), the extremely small size (15-30 mg) of the mouse lymph nodes was prohibitive for transporter protein analyses, which requires at least 100 mg of tissue before initial homogenization. Therefore, we opted to evaluate gene expression in mice and NHPs. Since transporter expression was low across all species by both methods, it is unlikely that any appreciable transporter protein concentrations would have been found in mice even with an adequate supply of tissue. Also, our gene and protein analyses do not account for transporter activity. Future IHC analysis of transporter localization in lymph nodes will investigate whether the majority of transporters are localized to plasma membranes, nuclear membranes, or within cytosol (where they would be functionally inactive) (Giacomini *et al.*, 2010).

In conclusion, we measured ARV penetration and drug transporter expression in humanized mouse, NHP, and human lymph nodes to further characterize species differences in ARV pharmacology within this putative HIV reservoir. We also investigated the effect of infection status and sex on ARV penetration, and characterized the relationship between drug transporter expression and ARV penetration in the lymph node. Most notably, in NHPs and humans we found that lymph node ARV exposure was greater than or equal to plasma, and lymph node concentrations (with the exception of TFV and RAL) were well-predicted by those in plasma. We also found that mouse and NHP TFVdp:dATP ratios met or exceeded human EC_{90} efficacy targets

in lymph nodes. There was no effect of infection or sex on lymph node ARV penetration in any species. We also found low drug transporter expression in lymph nodes from all species, and no predictive relationships between transporter gene or protein expression and ARV exposure, indicating that drug distribution in lymph nodes may occur through passive mechanisms. Our future research will focus on other physiologic (protein binding, tissue fibrosis) or physiochemical (molecular weight, lipophilicity) factors that may contribute to altered drug penetration and distribution in this reservoir. Along with the findings presented here, these data will have important implications for future preclinical and clinical drug development studies of HIV therapies targeted to lymph nodes.

Acknowledgements

We would like to acknowledge the National Research Disease Interchange, and Dr. Howard Fox and Elizabeth Kulka of the National NeuroAIDS Tissue Consortium for providing the human tissue samples used in this study. Funding sources include: the National Institutes of Health, National Institute of Mental Health and National Institute of Neurological Disorders and Stroke: Manhattan HIV Brain Bank (MHBB) [U24MH100931], Texas NeuroAIDS Research Center (TNRC) [U24MH100930], National Neurological AIDS Bank (NNAB) [U24MH100929], California NeuroAIDS Tissue Network (CNTN) [U24MH100928], Data Coordinating Center (DCC) [U24MH100925].

Authorship Contributions

Participated in research design: Fallon, Luciw, Garcia, Akkina, Smith, and Kashuba.

Conducted experiments: Burgunder, Fallon, White, Schauer, Sykes, Mulder, Kovarova, Adamson, Luciw, and Akkina.

Contributed new reagents or analytic tools: Smith.

Performed data analysis: Burgunder and Garcia.

Wrote or contributed to the writing of the manuscript: Burgunder and Kashuba.

References

Alam C, Whyte-Allman S-K, Omeragic A, and Bendayan R (2016) Role and modulation of drug transporters in HIV-1 therapy. *Adv Drug Deliv Rev* **103**:121–143.

Anderson PL, Kiser JJ, Gardner EM, Rower JE, Meditz A, and Grant RM (2011) Pharmacological considerations for tenofovir and emtricitabine to prevent HIV infection. *J Antimicrob Chemother* **66**:240–250.

Antonelli G, Turriziani O, Cianfriglia M, Riva E, Dong G, Fattorossi A, and Dianzani F (1992) Resistance of HIV-1 to AZT might also involve the cellular expression of multidrug resistance P-glycoprotein. *AIDS Res Hum Retroviruses* **8**:1839–1844.

Buzón MJ, Codoñer FM, Frost SDW, Pou C, Puertas MC, Massanella M, Dalmau J, Llibre JM, Stevenson M, Blanco J, Clotet B, Paredes R, and Martinez-Picado J (2011) Deep molecular characterization of HIV-1 dynamics under suppressive HAART. *PLoS Pathog* **7**:e1002314.

Chun TW, Davey RT, Engel D, Lane HC, and Fauci AS (1999) Re-emergence of HIV after stopping therapy. *Nature* **401**:874–875.

Cottrell ML, Yang KH, Prince HMA, Sykes C, White N, Malone S, Dellon ES, Madanick RD, Shaheen NJ, Hudgens MG, Wulff J, Patterson KB, Nelson JAE, and Kashuba ADM (2016) A translational pharmacology approach to predicting outcomes of preexposure prophylaxis against HIV in men and women using tenofovir disoproxil fumarate with or without emtricitabine. *J Infect Dis* **214**:55–64.

Deleage C, Wietgrefe SW, Del Prete G, Morcock DR, Hao XP, Piatak M, Bess J, Anderson JL, Perkey KE, Reilly C, McCune JM, Haase AT, Lifson JD, Schacker TW, and Estes JD (2016) Defining HIV and SIV reservoirs in lymphoid tissues. *Pathogens & immunity* **1**:68–106.

Denton PW, and García JV (2011) Humanized mouse models of HIV infection. *AIDS Rev* **13**:135–148.

Denton PW, Krisko JF, Powell DA, Mathias M, Kwak YT, Martinez-Torres F, Zou W, Payne DA, Estes JD, and Garcia JV (2010) Systemic administration of antiretrovirals prior to exposure prevents rectal and intravenous HIV-1 transmission in humanized BLT mice. *PLoS ONE* **5**:e8829.

Dimopoulos Y, Moysi E, and Petrovas C (2017) The lymph node in HIV pathogenesis. *Curr HIV/AIDS Rep* **14**:133–140.

Dumond JB, Patterson KB, Pecha AL, Werner RE, Andrews E, Damle B, Tressler R, Worsley J, and Kashuba ADM (2009) Maraviroc concentrates in the cervicovaginal fluid and vaginal tissue of HIV-negative women. *J Acquir Immune Defic Syndr* **51**:546–553.

Dumond JB, Yeh RF, Patterson KB, Corbett AH, Jung BH, Rezk NL, Bridges AS, Stewart PW, Cohen MS, and Kashuba ADM (2007) Antiretroviral drug exposure in the female genital tract: implications for oral pre- and post-exposure prophylaxis. *AIDS* **21**:1899–1907.

Else LJ, Taylor S, Back DJ, and Khoo SH (2011) Pharmacokinetics of antiretroviral drugs in anatomical sanctuary sites: the male and female genital tract. *Antivir Ther (Lond)* **16**:1149–1167.

Estes JD, Kityo C, Ssali F, Swainson L, Makamdop KN, Del Prete GQ, Deeks SG, Luciw PA, Chipman JG, Beilman GJ, Hoskuldsson T, Khoruts A, Anderson J, Deleage C, Jasurda J, Schmidt TE, Hafertepe M, Callisto SP, Pearson H, Reimann T, Schuster J, Schoephoerster J, Southern P, Perkey K, Shang L, Wietgrefe SW, Fletcher CV, Lifson JD, Douek DC, McCune JM, Haase AT, and Schacker TW (2017) Defining total-body AIDS-virus burden with implications for curative strategies. *Nat Med* **23**:1271–1276.

Evans DT, and Silvestri G (2013) Nonhuman primate models in AIDS research. *Curr Opin HIV AIDS* **8**:255–261.

Fallon JK, Neubert H, Hyland R, Goosen TC, and Smith PC (2013) Targeted quantitative proteomics for the analysis of 14 UGT1As and -2Bs in human liver using NanoUPLC-MS/MS with selected reaction monitoring. *J Proteome Res* **12**:4402–4413.

Fallon JK, Smith PC, Xia CQ, and Kim M-S (2016) Quantification of Four Efflux Drug Transporters in Liver and Kidney Across Species Using Targeted Quantitative Proteomics by Isotope Dilution NanoLC-MS/MS. *Pharm Res* **33**:2280–2288.

Fischman AJ, Babich JW, Bonab AA, Alpert NM, Vincent J, Callahan RJ, Correia JA, and Rubin RH (1998) Pharmacokinetics of [18F]trovafloxacin in healthy human subjects studied with positron emission tomography. *Antimicrob Agents Chemother* **42**:2048–2054.

Fletcher CV (2018) Comparative Lymphoid Tissue Pharmacokinetics (PK) of Integrase Inhibitors (INSTI) [2018 CROI Abstract 27].

Fletcher CV, Jiang H, Brundage RC, Acosta EP, Haubrich R, Katzenstein D, and Gulick RM (2004) Sex-based differences in saquinavir pharmacology and virologic response in AIDS Clinical Trials Group Study 359. *J Infect Dis* **189**:1176–1184.

Fletcher CV, Staskus K, Wietgrefe SW, Rothenberger M, Reilly C, Chipman JG, Beilman GJ, Khoruts A, Thorkelson A, Schmidt TE, Anderson J, Perkey K, Stevenson M, Perelson AS, Douek DC, Haase AT, and Schacker TW (2014) Persistent HIV-1 replication is associated with lower antiretroviral drug concentrations in lymphatic tissues. *Proc Natl Acad Sci U S A* **111**:2307–2312.

García-Lerma JG, Aung W, Cong M, Zheng Q, Youngpairoj AS, Mitchell J, Holder A, Martin A, Kuklenyik S, Luo W, Lin CY-C, Hanson DL, Kersh E, Pau C-P, Ray AS, Rooney JF, Lee WA, and Heneine W (2011) Natural substrate concentrations can modulate the prophylactic efficacy of nucleotide HIV reverse transcriptase inhibitors. *J Virol* **85**:6610–6617.

Giacomini KM, Huang SM, Tweedie DJ, Benet LZ, Brouwer KL, Chu X, Dahlin A, Evers R, Fischer V, Hillgren KM, Hoffmaster KA, Ishikawa T, Keppler D, Kim RB, Lee CA, Niemi M, Polli JW, Sugiyama Y, Swaan PW, Ware JA, Wright SH, Yee SW, Zamek-Gliszczynski MJ, and Zhang L (2010) Membrane transporters in drug development. *Nat Rev Drug Discov* **9**:215–236.

Gilead Sciences, Inc. (2001) VIREAD [package insert].

Giraud C, Manceau S, and Treluyer J-M (2010) ABC transporters in human lymphocytes: expression, activity and role, modulating factors and consequences for antiretroviral therapies. *Expert Opin Drug Metab Toxicol* **6**:571–589.

Goodman M, and Weigle W (1983) Activation of lymphocytes by a thiol-derivatized nucleoside: characterization of cellular parameters and responsive subpopulations. *The Journal of Immunology* **130**:551–557.

Goodman MG, and Weigle WO (1984) Intracellular lymphocyte activation and carrier-mediated transport of C8-substituted guanine ribonucleosides. *Proc Natl Acad Sci U S A* **81**:862–866.

Halvas E (2019) Nonsuppressible Viremia on ART from Large Cell Clones Carrying Intact Proviruses [2019 CROI Abstract 23].

Horiike M, Iwami S, Kodama M, Sato A, Watanabe Y, Yasui M, Ishida Y, Kobayashi T, Miura T, and Igarashi T (2012) Lymph nodes harbor viral reservoirs that cause rebound of plasma viremia in SIV-infected macaques upon cessation of combined antiretroviral therapy. *Virology* **423**:107–118.

Huang Y, Hoque MT, Jenabian M-A, Vyboh K, Whyte S-K, Sheehan NL, Brassard P, Bélanger M, Chomont N, Fletcher CV, Routy J-P, and Bendayan R (2016) Antiretroviral drug transporters and metabolic enzymes in human testicular tissue: potential contribution to HIV-1 sanctuary site. *J Antimicrob Chemother* **71**:1954–1965.

Kinman L, Brodie SJ, Tsai CC, Bui T, Larsen K, Schmidt A, Anderson D, Morton WR, Hu S-L, and Ho RJY (2003) Lipid-drug association enhanced HIV-1 protease inhibitor indinavir localization in lymphoid tissues and viral load reduction: a proof of concept study in HIV-2287-infected macaques. *J Acquir Immune Defic Syndr* **34**:387–397.

Kis O, Sankaran-Walters S, Hoque MT, Walmsley SL, Dandekar S, and Bendayan R (2016) HIV-1 Alters Intestinal Expression of Drug Transporters and Metabolic Enzymes:

Implications for Antiretroviral Drug Disposition. *Antimicrob Agents Chemother* **60**:2771–2781.

Kwara A, Delong A, Rezk N, Hogan J, Burtwell H, Chapman S, Moreira CC, Kurpewski J, Ingersoll J, Caliendo AM, Kashuba A, and Cu-Uvin S (2008) Antiretroviral drug concentrations and HIV RNA in the genital tract of HIV-infected women receiving long-term highly active antiretroviral therapy. *Clin Infect Dis* **46**:719–725.

Lamers SL, Rose R, Maidji E, Agsalda-Garcia M, Nolan DJ, Fogel GB, Salemi M, Garcia DL, Bracci P, Yong W, Commins D, Said J, Khanlou N, Hinkin CH, Sueiras MV, Mathisen G, Donovan S, Shiramizu B, Stoddart CA, McGrath MS, and Singer EJ (2016) HIV DNA Is Frequently Present within Pathologic Tissues Evaluated at Autopsy from Combined Antiretroviral Therapy-Treated Patients with Undetectable Viral Loads. *J Virol* **90**:8968–8983.

Lewin SR, and Rouzioux C (2011) HIV cure and eradication: how will we get from the laboratory to effective clinical trials? *AIDS* **25**:885–897.

Lorenzo-Redondo R, Fryer HR, Bedford T, Kim E-Y, Archer J, Pond SLK, Chung Y-S, Penugonda S, Chipman J, Fletcher CV, Schacker TW, Malim MH, Rambaut A, Haase AT, McLean AR, and Wolinsky SM (2016) Persistent HIV-1 replication maintains the tissue reservoir during therapy. *Nature* **530**:51–56.

Massud I, Aung W, Martin A, Bachman S, Mitchell J, Aubert R, Solomon Tsegaye T, Kersh E, Pau C-P, Heneine W, and García-Lerma JG (2013) Lack of prophylactic efficacy of oral maraviroc in macaques despite high drug concentrations in rectal tissues. *J Virol* **87**:8952–8961.

Minuesa G, Huber-Ruano I, Pastor-Anglada M, Koepsell H, Clotet B, and Martinez-Picado J (2011) Drug uptake transporters in antiretroviral therapy. *Pharmacol Ther* **132**:268–279.

Minuesa G, Purcet S, Erkizia I, Molina-Arcas M, Bofill M, Izquierdo-Useros N, Casado FJ, Clotet B, Pastor-Anglada M, and Martinez-Picado J (2008) Expression and functionality of anti-

human immunodeficiency virus and anticancer drug uptake transporters in immune cells. *J Pharmacol Exp Ther* **324**:558–567.

Natarajan V, Bosche M, Metcalf JA, Ward DJ, Lane HC, and Kovacs JA (1999) HIV-1 replication in patients with undetectable plasma virus receiving HAART. Highly active antiretroviral therapy. *The Lancet* **353**:119–120.

Neff CP, Ndolo T, Tandon A, Habu Y, and Akkina R (2010) Oral pre-exposure prophylaxis by anti-retrovirals raltegravir and maraviroc protects against HIV-1 vaginal transmission in a humanized mouse model. *PLoS ONE* **5**:e15257.

Nicol MR, Fedoriw Y, Mathews M, Prince HMA, Patterson KB, Geller E, Mollan K, Mathews S, Kroetz DL, and Kashuba ADM (2014) Expression of six drug transporters in vaginal, cervical, and colorectal tissues: Implications for drug disposition in HIV prevention. *J Clin Pharmacol* **54**:574–583.

North TW, Higgins J, Deere JD, Hayes TL, Villalobos A, Adamson L, Shacklett BL, Schinazi RF, and Luciw PA (2010) Viral sanctuaries during highly active antiretroviral therapy in a nonhuman primate model for AIDS. *J Virol* **84**:2913–2922.

Ohtsuki S, Schaefer O, Kawakami H, Inoue T, Liehner S, Saito A, Ishiguro N, Kishimoto W, Ludwig-Schwellinger E, Ebner T, and Terasaki T (2012) Simultaneous absolute protein quantification of transporters, cytochromes P450, and UDP-glucuronosyltransferases as a novel approach for the characterization of individual human liver: comparison with mRNA levels and activities. *Drug Metab Dispos* **40**:83–92.

Patterson KB, Prince HA, Kraft E, Jenkins AJ, Shaheen NJ, Rooney JF, Cohen MS, and Kashuba ADM (2011) Penetration of tenofovir and emtricitabine in mucosal tissues: implications for prevention of HIV-1 transmission. *Sci Transl Med* **3**:112re4.

Samji H, Cescon A, Hogg RS, Modur SP, Althoff KN, Buchacz K, Burchell AN, Cohen M, Gebo KA, Gill MJ, Justice A, Kirk G, Klein MB, Korthuis PT, Martin J, Napravnik S, Rourke SB, Sterling TR, Silverberg MJ, Deeks S, Jacobson LP, Bosch RJ, Kitahata MM, Goedert JJ,

Moore R, Gange SJ, and North American AIDS Cohort Collaboration on Research and Design (NA-ACCORD) of IeDEA (2013) Closing the gap: increases in life expectancy among treated HIV-positive individuals in the United States and Canada. *PLoS ONE* **8**:e81355.

Schmittgen TD, and Livak KJ (2008) Analyzing real-time PCR data by the comparative CT method. *Nat Protoc* **3**:1101–1108.

Shytaj IL, Norelli S, Chirullo B, Della Corte A, Collins M, Yalley-Ogunro J, Greenhouse J, Iraci N, Acosta EP, Barreca ML, Lewis MG, and Savarino A (2012) A highly intensified ART regimen induces long-term viral suppression and restriction of the viral reservoir in a simian AIDS model. *PLoS Pathog* **8**:e1002774.

Solas C, Lafeuillade A, Halfon P, Chadapaud S, Hittinger G, and Lacarelle B (2003) Discrepancies between protease inhibitor concentrations and viral load in reservoirs and sanctuary sites in human immunodeficiency virus-infected patients. *Antimicrob Agents Chemother* **47**:238–243.

Speck RR, Yu X-F, Hildreth J, and Flexner C (2002) Differential effects of p-glycoprotein and multidrug resistance protein-1 on productive human immunodeficiency virus infection. *J Infect Dis* **186**:332–340.

Srinivas N (2018) Doctoral Dissertation, Distribution of Antiretrovirals within the Brain Tissue and Relationship with Neurocognitive Impairment Due to HIV, The University of North Carolina at Chapel Hill.

Srinivas N, Rosen EP, Gilliland WM, Kovarova M, Remling-Mulder L, De La Cruz G, White N, Adamson L, Schauer AP, Sykes C, Luciw P, Garcia JV, Akkina R, and Kashuba ADM (2018) Antiretroviral concentrations and surrogate measures of efficacy in the brain tissue and CSF of preclinical species. *Xenobiotica* 1–10.

Thompson CG (2017) Doctoral Dissertation, Tissue Reservoir of HIV: Implications for Eradication, The University of North Carolina at Chapel Hill.

Thompson CG, Bokhart MT, Sykes C, Adamson L, Fedoriw Y, Luciw PA, Muddiman DC, Kashuba ADM, and Rosen EP (2015) Mass spectrometry imaging reveals heterogeneous efavirenz distribution within putative HIV reservoirs. *Antimicrob Agents Chemother* **59**:2944–2948.

Thompson CG, Fallon JK, Mathews M, Charlins P, Remling-Mulder L, Kovarova M, Adamson L, Srinivas N, Schauer A, Sykes C, Luciw P, Garcia JV, Akkina R, Smith PC, and Kashuba ADM (2017) Multimodal analysis of drug transporter expression in gastrointestinal tissue. *AIDS* **31**:1669–1678.

Van Loo PLP, Van Zutphen LFM, and Baumans V (2003) Male management: Coping with aggression problems in male laboratory mice. *Lab Anim* **37**:300–313.

Veselinovic M, Yang K-H, LeCureux J, Sykes C, Remling-Mulder L, Kashuba ADM, and Akkina R (2014) HIV pre-exposure prophylaxis: mucosal tissue drug distribution of RT inhibitor Tenofovir and entry inhibitor Maraviroc in a humanized mouse model. *Virology* **464-465**:253–263.

Zhou T, Hu M, Cost M, Poloyac S, and Rohan L (2013) Short communication: expression of transporters and metabolizing enzymes in the female lower genital tract: implications for microbicide research. *AIDS Res Hum Retroviruses* **29**:1496–1503.

Footnotes

[§]This work was supported by the National Institutes of Health, National Institute of Allergy and Infectious Diseases [Grant AI111891]; the University of North Carolina at Chapel Hill Center for AIDS Research (UNC CFAR) [Grant P30 AI50410]; the California National Primate Research Center [Grant P51 OD011107]. Its contents are solely the responsibility of the authors and do not necessarily represent the official view of the NIH.

JPET Fast Forward. Published on June 24, 2019 as DOI: 10.1124/jpet.119.259150
This article has not been copyedited and formatted. The final version may differ from this version.

Figure Legends

Figure 1. Cross-species differences in ARV concentrations in (A) plasma (ng/ml) and (B) lymph nodes (ng/g tissue) from mice (blue boxes), NHPs (purple boxes), and humans (green boxes). Boxes are the 25th percentile, median, and 75th percentile, whiskers are the 5th and 95th percentiles, and dots are outliers. Dashed lines indicate LLOQs. Sample sizes for each drug in each species are given in Supplemental Table 2. Between-species differences were analyzed using Kruskal-Wallis One-Way ANOVA with Dunn's Method correction for multiple comparisons. *p<0.05

Figure 2. Cross-species differences in ARV tissue penetration ratios (TPRs) in mice (blue boxes), NHPs (purple boxes), and humans (green boxes). Boxes are the 25th percentile, median, and 75th percentile, whiskers are the 5th and 95th percentiles, and dots are outliers. Dashed line indicates equal drug concentrations in lymph node and plasma. Sample sizes for each drug in each species are given in Supplemental Table 2. Between-species differences were analyzed using Kruskal-Wallis One-Way ANOVA with Dunn's Method correction for multiple comparisons. *p<0.05

Figure 3. Cross-species differences in (A) active metabolite and endogenous nucleotide concentrations (ng/g tissue), and (B) metabolite: nucleotide ratios in lymph nodes of mice (blue boxes), NHPs (purple boxes), and humans (green boxes). Boxes are the 25th percentile, median, and 75th percentile, whiskers are the 5th and 95th percentiles, and dots are outliers. Dashed lines in (A) indicate LLOQs, and in (B) equal metabolite and nucleotide concentrations. Sample sizes for each drug in each species are given in Supplemental Table 2. Between-species differences were analyzed using Kruskal-Wallis One-Way ANOVA with Dunn's Method correction for multiple comparisons. *p<0.05

Figure 4. Differences in ARV tissue penetration ratios (TPRs) in uninfected (gray boxes) and infected (red boxes) (A) mouse and (B) NHP lymph nodes. Boxes are the 25th percentile, median, and 75th percentile, whiskers are the 5th and 95th percentiles, and dots are outliers. Dashed line indicates equal drug concentrations in lymph node and plasma. Sample sizes for each drug in each species are given in Supplemental Table 2. Infection differences were analyzed using Kruskal-Wallis One-Way ANOVA with Dunn's Method correction for multiple comparisons.

Figure 5. Differences in ARV tissue penetration ratios (TPRs) in female (pink boxes) and male (blue boxes) (A) NHP and (B) human lymph nodes. Boxes are the 25th percentile, median, and 75th percentile, whiskers are the 5th and 95th percentiles, and dots are outliers. Dashed line indicates equal drug concentrations in lymph node and plasma. Sample sizes for each drug in each species are given in Supplemental Table 2. Sex differences were analyzed using Kruskal-Wallis One-Way ANOVA with Dunn's Method correction for multiple comparisons.

Figure 6. Cross-species differences in drug transporter expression in lymph nodes. (A) Gene expression (measured as the fold change over the housekeeping gene GAPDH) of 8 drug transporters in the lymph nodes of mice (blue boxes) and NHPs (purple boxes). (B) Protein concentrations (pmol/mg protein) of 8 drug transporters in the lymph nodes of NHPs (purple boxes) and humans (green boxes). Boxes are the 25th percentile, median, and 75th percentile, whiskers are the 5th and 95th percentiles, and dots are outliers. Dashed lines in (A) represent the LLOQ, and in (B) the LLOD. Sample sizes for each species are given in Supplemental Table 2. Between-species differences were analyzed using Kruskal-Wallis One-Way ANOVA with Dunn's Method correction for multiple comparisons. *$p<0.05$

JPET Fast Forward. Published on June 24, 2019 as DOI: 10.1124/jpet.119.259150
This article has not been copyedited and formatted. The final version may differ from this version.

Tables

Table 1. Molar percent of FTC, FTCtp, TFV, and TFVdp in mouse, NHP, and human lymph nodes. Data are median (min, max) molar percentage.

ARV	Mouse	NHP	Human
FTC mol %	99.8 (77.4, 100)	95.2 (79, 100)	98.9 (2.1, 100)
FTCtp mol %	0.2 (0, 22.6)	4.8 (0, 21)	1.1 (0, 97.9)
TFV mol %	99.9 (95.6, 100)	93.6 (64.2, 100)	99.8 (89.3, 100)
TFVdp mol %	0.1 (0, 4.4)	6.4 (0, 35.8)	0.2 (0, 10.7)

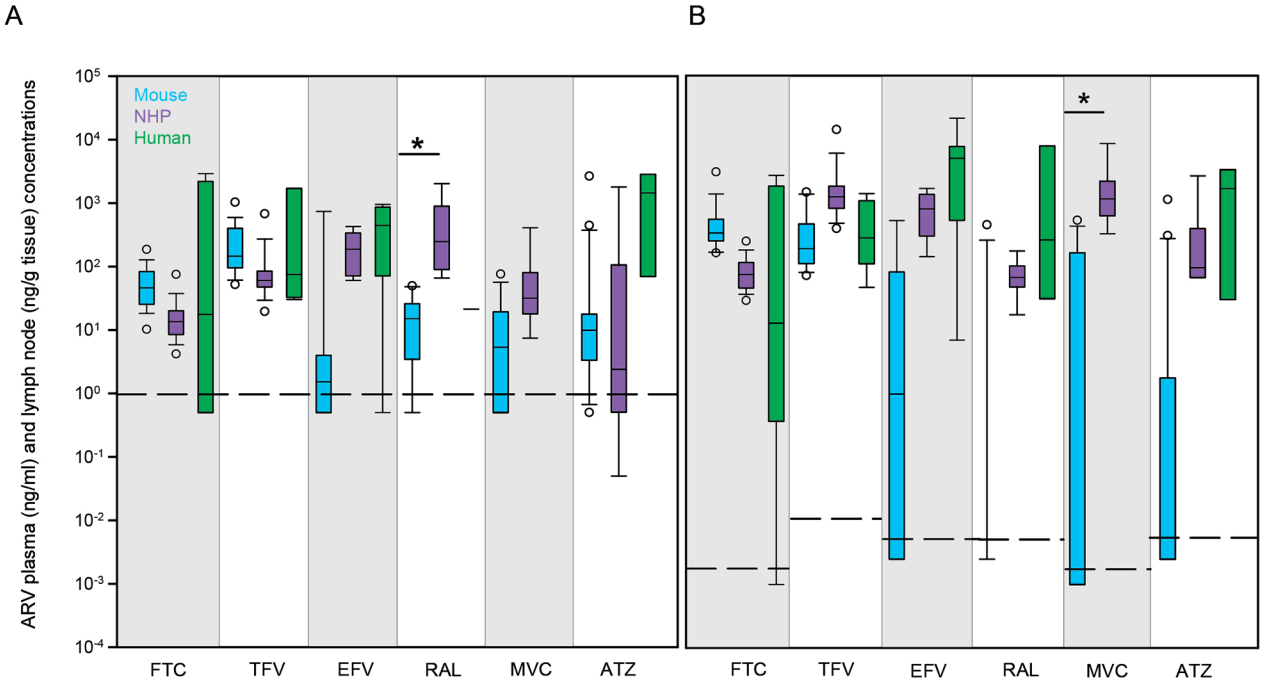
A
B
Mouse
NHP
Human
ARV plasma (ng/ml) and lymph node (ng/g tissue) concentrations
10^5
10^4
10^3
10^2
10^1
10^0
10^{-1}
10^{-2}
10^{-3}
10^{-4}
*
*
FTC
TFV
EFV
RAL
MVC
ATZ
FTC
TFV
EFV
RAL
MVC
ATZ

Figure 1

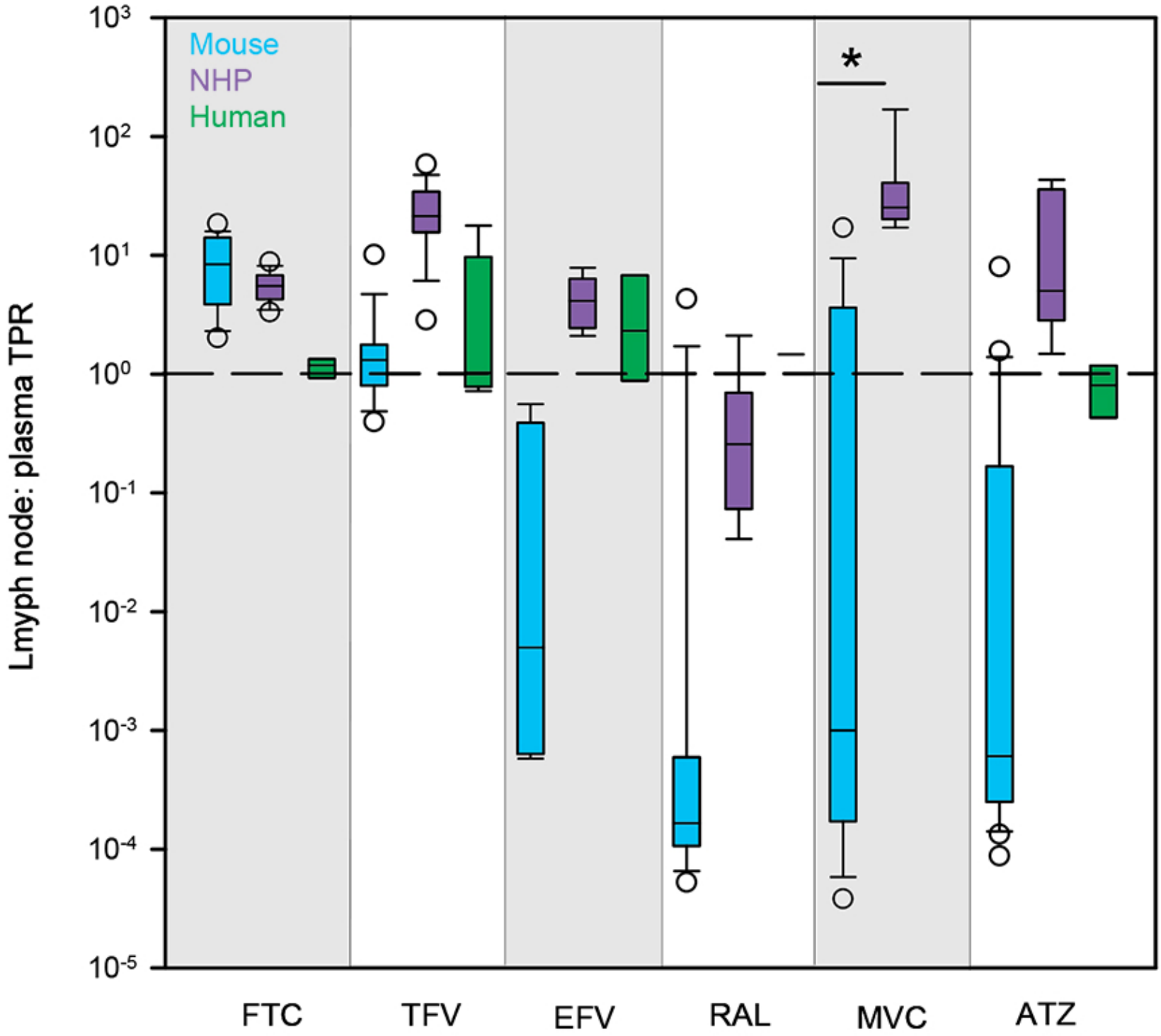
Mouse
NHP
Human
Lmyph node: plasma TPR
10^3
10^2
10^1
10^0
10^{-1}
10^{-2}
10^{-3}
10^{-4}
10^{-5}
*
FTC
TFV
EFV
RAL
MVC
ATZ

Figure 2

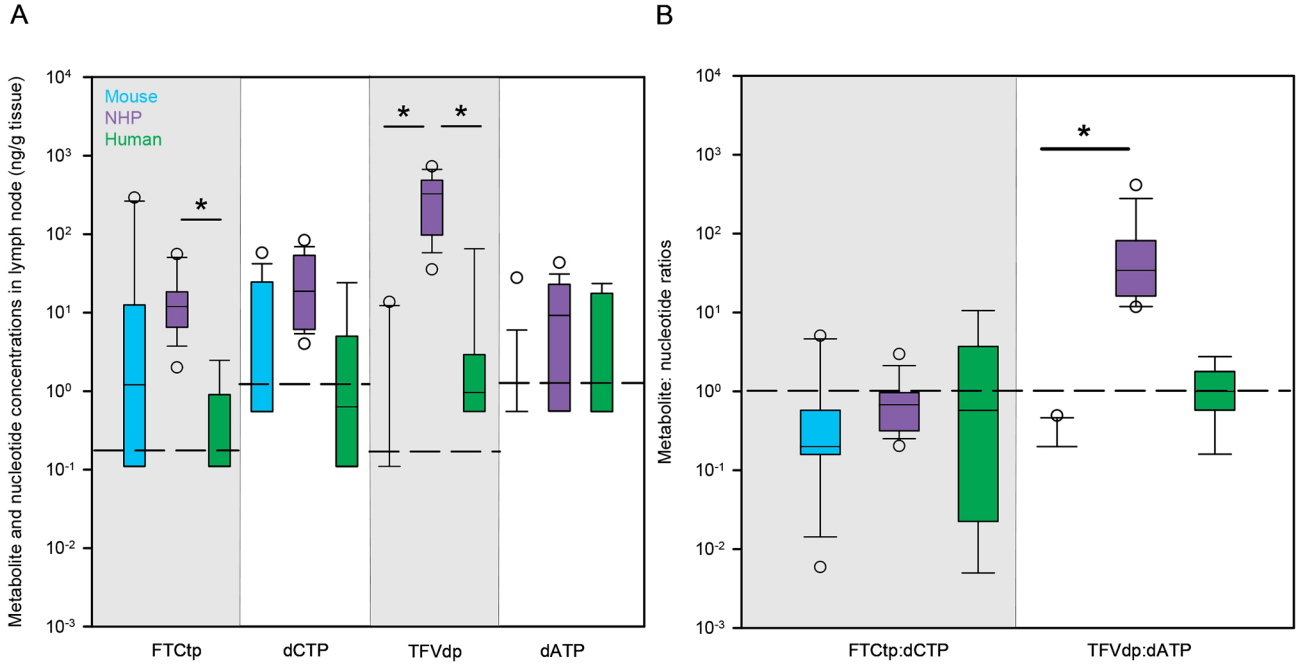
A
B
Mouse
NHP
Human
Metabolite and nucleotide concentrations in lymph node (ng/g tissue)
Metabolite: nucleotide ratios
FTCtp
dCTP
TFVdp
dATP
FTCtp:dCTP
TFVdp:dATP
*

Figure 3

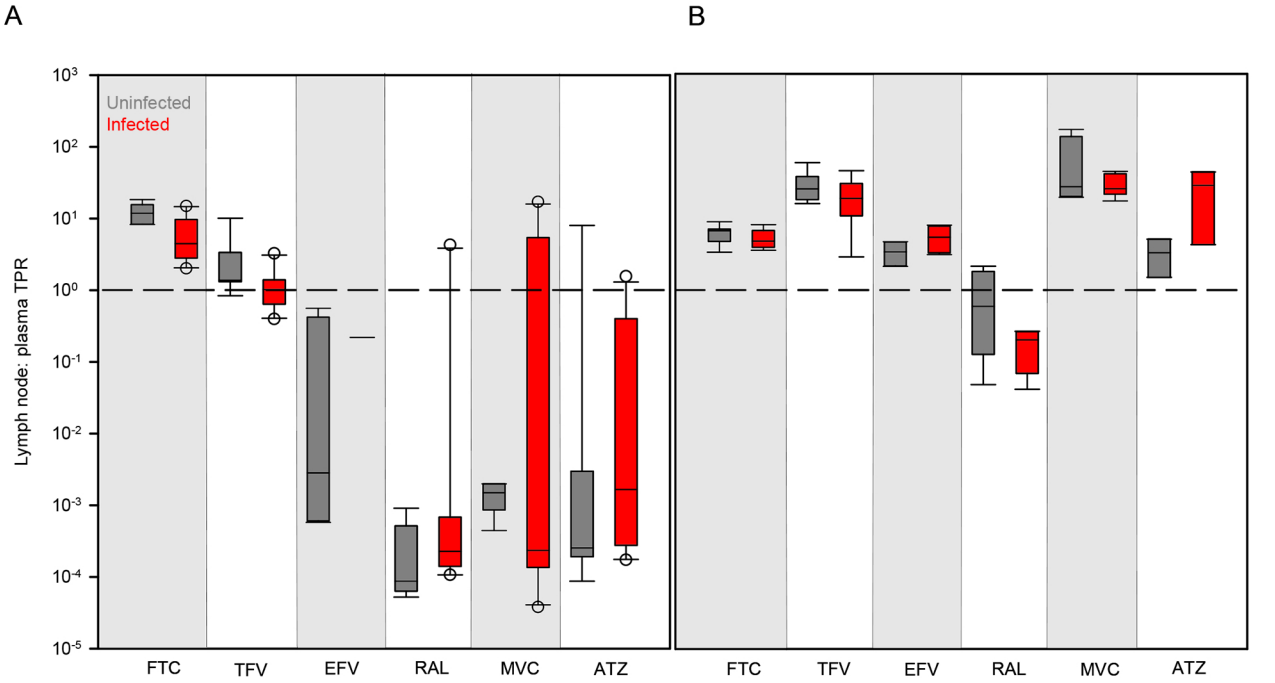
A
B
Uninfected
Infected
Lymph node: plasma TPR
10^{3}
10^{2}
10^{1}
10^{0}
10^{-1}
10^{-2}
10^{-3}
10^{-4}
10^{-5}
FTC
TFV
EFV
RAL
MVC
ATZ

Figure 4

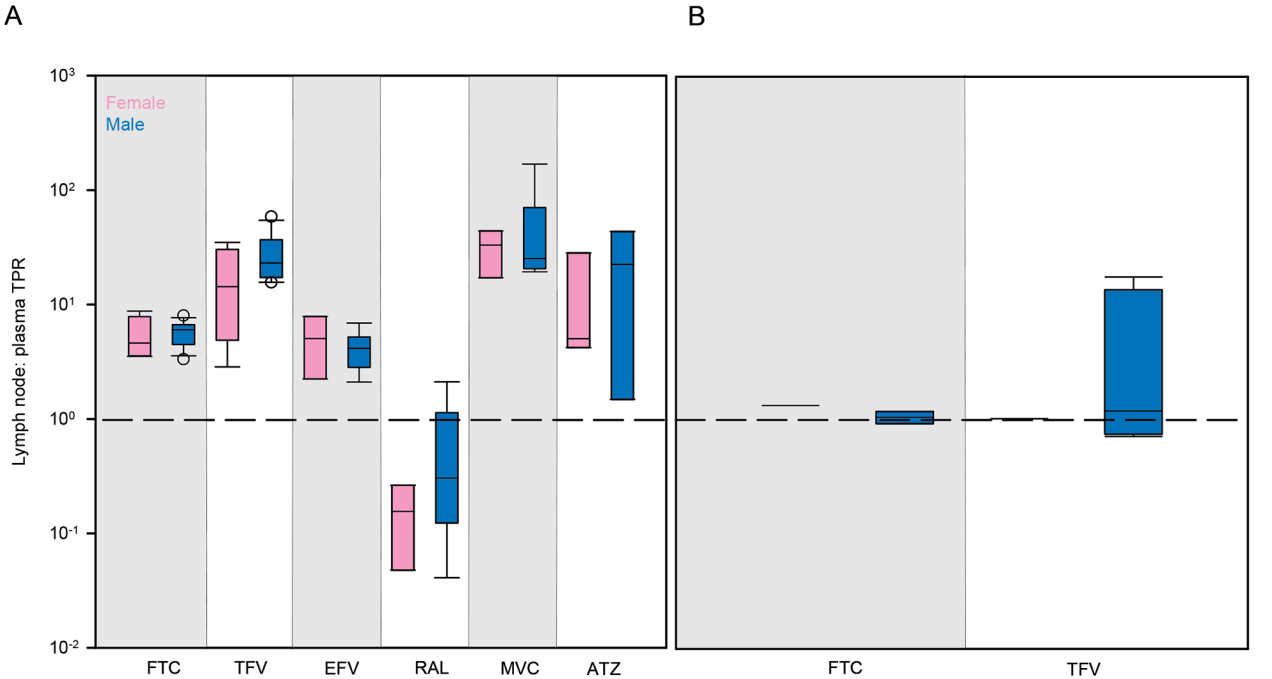
A
B
Female
Male
Lymph node: plasma TPR
10^3
10^2
10^1
10^0
10^{-1}
10^{-2}
FTC
TFV
EFV
RAL
MVC
ATZ
FTC
TFV

Figure 5

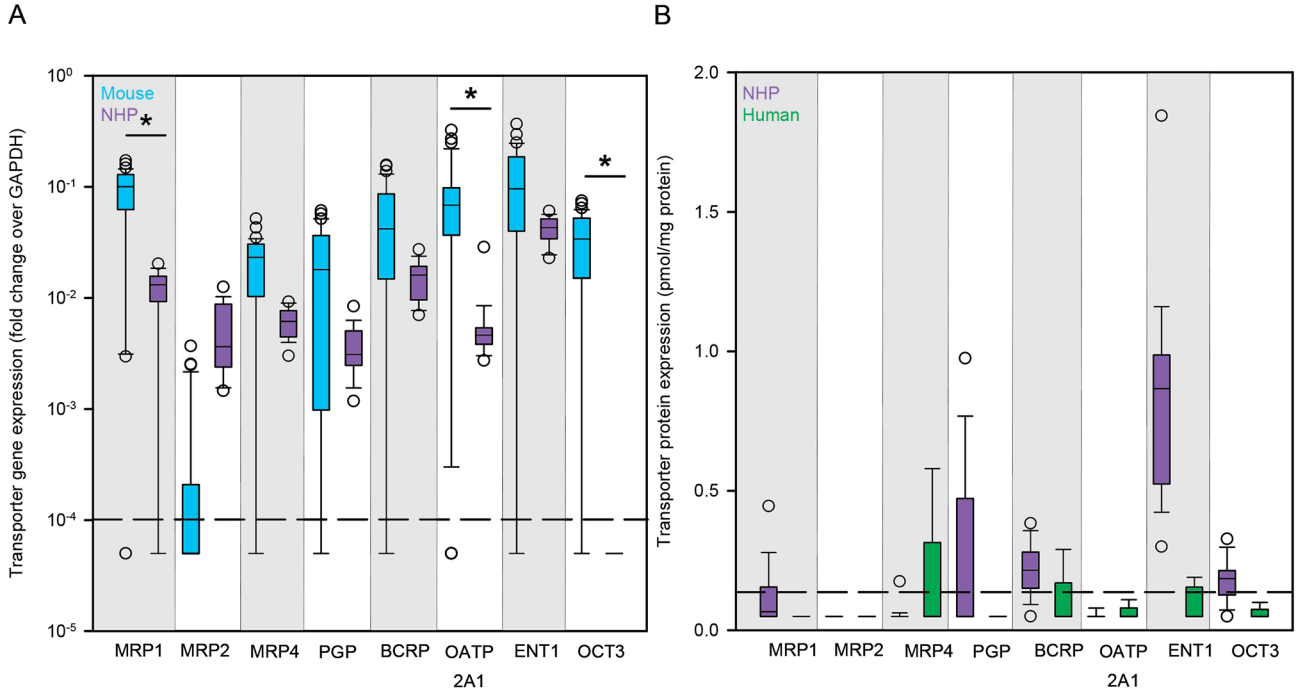
A
B
Mouse
NHP
Human
Transporter gene expression (fold change over GAPDH)
Transporter protein expression (pmol/mg protein)
MRP1
MRP2
MRP4
PGP
BCRP
OATP
ENT1
OCT3
2A1
*

Figure 6

The Journal of Pharmacology and Experimental Therapeutics

Antiretroviral drug concentrations in lymph nodes: a cross-species comparison of the effect of drug transporter expression, viral infection, and sex in humanized mice, nonhuman primates, and humans

Erin Burgunder, John K. Fallon, Nicole White, Amanda Schauer, Craig Sykes, Leila Remling-Mulder, Martina Kovarova, Lourdes Adamson, Paul Luciw, J. Victor Garcia, Ramesh Akkina, Philip C. Smith, and Angela DM Kashuba

Supplemental Data

Animal Studies: Dosing, Infection, Tissue Collection and Use

Uninfected Animals

hu-HSC-Rag (RagHu) humanized mice (n=18), bone marrow-liver-thymus (BLT) humanized mice (n=6), and non-human primates (NHPs) (n=8) were used as uninfected comparators in this study. All humanized mice and 2 NHPs were female.

RagHu mice aged 3-6 months were dosed orally (PO) once daily (QD) for 10 days with one of several antiretroviral (ARV) regimens: efavirenz (EFV, 10 mg/kg) alone, atazanavir (ATZ, 140 mg/kg) alone, or a combination of tenofovir (TFV, 208 mg/kg) + emtricitabine (FTC, 240 mg/kg) + raltegravir (RAL, 56 mg/kg) + maraviroc (MVC, 62 mg/kg). BLT mice received a combination of TFV, FTC, RAL, ATZ, and MVC at equivalent doses for 6 days. All drugs were administered by oral gavage, and dosing solutions were prepared by solubilizing formulated drug.

Rhesus macaques (*Macaca mulatta*) between 3 and 7 years of age were dosed for 10 days with one of the following regimens: TFV (30 mg/kg subcutaneously (SubQ) QD) + FTC (16 mg/kg SubQ QD) + EFV (200 mg PO QD) + RAL (100 mg PO BID), or TFV (30 mg/kg SubQ) + FTC (16mg/kg SubQ) + MVC (150 mg/kg PO BID) + ATZ (270 mg/kg PO BID). Dosing periods for all animals were chosen to achieve pharmacokinetic steady state in tissues based on known half-lives of the drugs used and previous studies with these models. Dosing regimen sample sizes for each animal model are summarized in Supplemental Table 1.

Infected Animals

RagHu mice (n=18), BLT mice (n=7), and NHPs (n=10) were used to assess the effect of infection on drug distribution and transporter expression. All mice and 4 NHPs were female.

RagHu mice were infected intraperitoneally with 200µL 2.1 x 10^6 IU/mL of $HIV_{Bal\ D7}$. Plasma HIV RNA was measured weekly beginning 2 weeks after inoculation and continuing for 4 weeks. ART dosing commenced once 4 weeks of durable HIV infection was established, and a final viral load was measured during therapy. BLT mice were infected intravenously with 200µL 90,000 TCIU of HIV_{JRcsf}, with plasma HIV RNA being measured 1, 2 and 4 weeks after inoculation to confirm durable infection, and once after starting therapy. NHPs were infected intravenously with $10^{4.5}$ $TCID_{50}$ of RT-SHIV, with viral loads measured weekly after inoculation. ART dosing commenced once 4 weeks of durable HIV infection was established, and a final viral load was measured during therapy. Infected animals were dosed with the same ART regimens detailed above, and are summarized in Supplemental Table 1.

Tissue Collection and Use

One day after the final ARV doses were administered, animals were euthanized by phenobarbital injection and underwent necropsy. Whole blood was collected via retro-orbital or cardiac puncture for mice and venipuncture for macaques. Several tissues suspected of being

HIV reservoirs were collected from all animals, including the lymph node. After removal from the body, tissues were placed into aluminum foil pouches and snap frozen on dry ice. Total time from euthanasia to tissue freezing was less than 60 minutes for all tissues. After freezing, tissues were stored at -80˚C for further analysis. Details on the use of lymph nodes and the sample size for each analysis are shown in Supplemental Table 2.

Dosing Regimen	**Mice** (all female)				**NHPs**	
	BLT		**RagHu**			
	+	**-**	**+**	**-**	**+**	**-**
EFV			N=6	N=6		
ATZ			N=6	N=6		
TFV/FTC/RAL/MVC			N=6	N=6		
TFV/FTC/RAL/MVC/ATZ	N=7	N=6				
TFV/FTC/EFV/RAL					N=5 (2 female)	N=4 (1 female)
TFV/FTC/MVC/ATZ					N=5 (2 female)	N=4 (1 female)

Supplemental Table 1: Preclinical animal dosing distribution

Species	**TFVdp, FTCtp, dATP, dCTP concentration**	**TFVdp:dATP, FTCtp:dCTP ratio**	**ARV concentration**	**ARV tissue penetration ratio (TPR)**	**Gene expression only**	**Matched gene expression + ARV TPR**	**Protein concentration only**	**Matched protein concentration + ARV TPR**
Mice								
N_{TOTAL}	17	10	36	32	33	24	N/A	N/A
$N_{INFECTION}$	8 (-) 9 (+)	5 (-) 5 (+)	17 (-) 19 (+)	16 (-) 16 (+)	13 (-) 20 (+)	10 (-) 14 (+)		
N_{SEX}	All (F)	All (F)	All (F)	All (F)	All (F)	All (F)		
N_{ARV}	10 (TFVdp) 10 (FTCtp) 17 (dATP) 17 (dCTP)	10 (TFVdp:dATP) 10 (FTCtp:dCTP)	17 (TFV) 17 (FTC) 9 (EFV) 17 (RAL) 17 (MVC) 21 (ATZ)	16 (TFV) 17 (FTC) 5 (EFV) 15 (RAL) 16 (MVC) 21 (ATZ)		15 (TFV) 15 (FTC) 2 (EFV) 14 (RAL) 15 (MVC) 18 (ATZ)		
NHPs								
N_{TOTAL}	16	16	17	17	18	17	18	17
$N_{INFECTION}$	8 (-) 8 (+)	8 (-) 8 (+)	8 (-) 9 (+)	8 (-) 9 (+)	8 (-) 10 (+)	8 (-) 9 (+)	8 (-) 10 (+)	8 (-) 9 (+)
N_{SEX}	11 (M) 5 (F)	11 (M) 5 (F)	12 (M) 5 (F)	12 (M) 5 (F)	12 (M) 6 (F)	12 (M) 5 (F)	12 (M) 6 (F)	12 (M) 5 (F)
N_{ARV}	16 (TFVdp) 16 (FTCtp) 16 (dATP) 16 (dCTP)	16 (TFVdp:dATP) 16 (FTCtp:dCTP)	17 (TFV) 17 (FTC) 8 (EFV) 8 (RAL) 9 (MVC) 9 (ATZ)	17 (TFV) 17 (FTC) 8 (EFV) 8 (RAL) 9 (MVC) 5 (ATZ)		17 (TFV) 17 (FTC) 8 (EFV) 8 (RAL) 9 (MVC) 5 (ATZ)		12 (M) 5 (F) 17 (TFV) 17 (FTC) 8 (EFV) 8 (RAL) 9 (MVC) 5 (ATZ)
Humans								
N_{TOTAL}	8	8	13	6	N/A	N/A	5	1
$N_{INFECTION}$	All (+)	All (+)	All (+)	All (+)			All (+)	All (+)
N_{SEX}	7 (M) 1 (F)	7 (M) 1 (F)	11 (M) 2 (F)	5 (M) 1 (F)			4 (M) 1 (F)	1 (M) 0 (F)
N_{ARV}	8 (TFVdp) 8 (FTCtp) 8 (dATP) 8 (dCTP)	8 (TFVdp:dATP) 8 (FTCtp:dCTP)	11 (M) 2 (F) 8 (TFV) 8 (FTC) 7 (EFV) 3 (RAL) 0 (MVC) 2 (ATZ)	5 (M) 1 (F) 5 (TFV) 3 (FTC) 3 (EFV) 1 (RAL) 0 (MVC) 2 (ATZ)				1 (M) 0 (F) 1 (TFV) 1 (FTC) 0 (EFV) 0 (RAL) 0 (MVC) 1 (ATZ)

Supplemental Table 2: Sample sizes for each analysis

Sample ID	ARV plasma concentration (ng/g)	Post-mortem interval (hrs)	Pre-mortem viral load (cp/ml)	Pre-mortem CD4 count (cells/ml)	Gender	Race	Age at Death (yrs)	Years with HIV
HV00103-13	TFV: N/A FTC: N/A EFV: N/A	7.5	<50	269	M	Black	57	5
HV00119-10	TFV: N/A FTC: N/A	6.5	<50	175	M	Black	45	Unknown
7102547787	TFV: 74.9 FTC: 17.6 RAL: 21.3	25.2	20	8	F	Black	55	7
1077	TFV: 30.3 FTC: BLQ EFV: 284	6	2760	142	M	White	47	1
1117	EFV: BLQ	24.5	37060	114	F	Black	55	16
4077	TFV: 1660 FTC: 1440 ATZ: 69.8	6	402	3	M	White	34	10
6081	TFV: 1720 FTC: 2920 ATZ: 2830	2	Unknown	Unknown	M	White	35	10
MHBB708*	RAL: N/A	23	<50	88	M	Black	63	Unknown
MHBB716*	TFV: N/A FTC: N/A EFV: N/A	47	<50	597	M	Black	67	Unknown
MHBB725*	EFV: N/A	22	<50	106	M	Unknown	60	21
MHBB731*	RAL: N/A	40.5	<50	503	M	White	73	24
10015	EFV: 953	20	176800	66	M	White	34	8
10067	TFV: 35.3 FTC: BLQ EFV: 606	8	2097	5	M	Asian	27	12

*witnessed dosing

Supplemental Table 3: Patient characteristics and ARV regimens

Transport Direction	Gene Name	Protein Name	ARV Substrates	ARV Inhibitors	ARV Inducers
Efflux	Abcc1	MRP1	FTC, ATZ	FTC, TFV, EFV	
Efflux	Abcc2	MRP2	TFV, ATZ	FTC, TFV, EFV	MVC
Efflux	Abcc4	MRP4	TFV		
Efflux	Abcb1	PGP	RAL, MVC, ATZ	FTC, EFV, MVC, ATZ	FTC, EFV, ATZ
Efflux	Abcg2	BCRP	TFV, EFV, RAL	EFV, ATZ	
Uptake	Slco2A1	OATP2A1	ATZ	ATZ	
Uptake	Slc29A1	ENT1	FTC, TFV		
Uptake	Slc22A3	OCT3	Lamivudine (3TC)		

Supplemental Table 4: Drug transporters used in gene and protein expression analyses

Gene Name	Species	Catalog Number
ABCB1	Mouse	Mm00440736_m1
ABCC1	Mouse	Mm00456156_m1
ABCC2	Mouse	Mm00496899_m1
ABCC4	Mouse	Mm01226381_m1
ABCG2	Mouse	Mm00496364_m1
SLCO2A1	Mouse	Mm00459638_m1
SLC29A1	Mouse	Mm01270577_m1
SLC22A3	Mouse	Mm00488294_m1
GAPDH	Mouse	Mm99999915_g1
ABCB1	Macaque	Rh02788239_m1
ABCC1	Macaque	Hs01561502_m1
ABCC2	Macaque	Rh02788077_m1
ABCC4	Macaque	Rh02858818_m1
ABCG2	Macaque	Rh02788848_m1
SLCO2A1	Macaque	Rh02858210_m1
SLC29A1	Macaque	Rh02794207_m1
SLC22A3	Macaque	Hs01009568_m1
GAPDH	Macaque	Rh02621745_g1

Supplemental Table 5: Taqman gene expression assays used in mice and NHPs

Gene	FTC TPR	TFV TPR	EFV TPR	RAL TPR	MVC TPR	ATZ TPR
Transporters tested	MRP1 MRP2 PGP	MRP1 MRP2 MRP4 BCRP ENT1	PGP BCRP	PGP BCRP	MRP2 PGP OATP2A1	MRP1 MRP2 PGP BCRP OATP2A1
Intercept	6.6	7.1	4.9	0.39	18	5.4
Significant transporter coefficient(s)	none	MRP2: 2290 (p=0.002)	none	none	none	none
R^2	0.14	0.27	0.39	0.02	0.20	0.10

Supplemental Table 6: Multilinear regression analysis of the influence of drug transporter gene expression on ARV penetration in mouse and NHP lymph nodes

Gene	FTC TPR	TFV TPR	EFV TPR	RAL TPR	MVC TPR	ATZ TPR
Transporters tested	MRP1 MRP2 PGP	MRP1 MRP2 MRP4 BCRP ENT1	PGP BCRP	PGP BCRP	MRP2 PGP OATP2A1	MRP1 MRP2 PGP BCRP OATP2A1
Intercept	4.9	15	0.56	1.5	76	-7.0
Significant transporter coefficient(s)	none	none	none	none	none	MRP1: 105 (p<0.001) PGP: 74 (p<0.001)
R^2	0.10	0.34	0.42	0.23	0.02	0.99

Supplemental Table 7: Multilinear regression analysis of the influence of drug transporter protein expression on ARV penetration in NHP and human lymph nodes

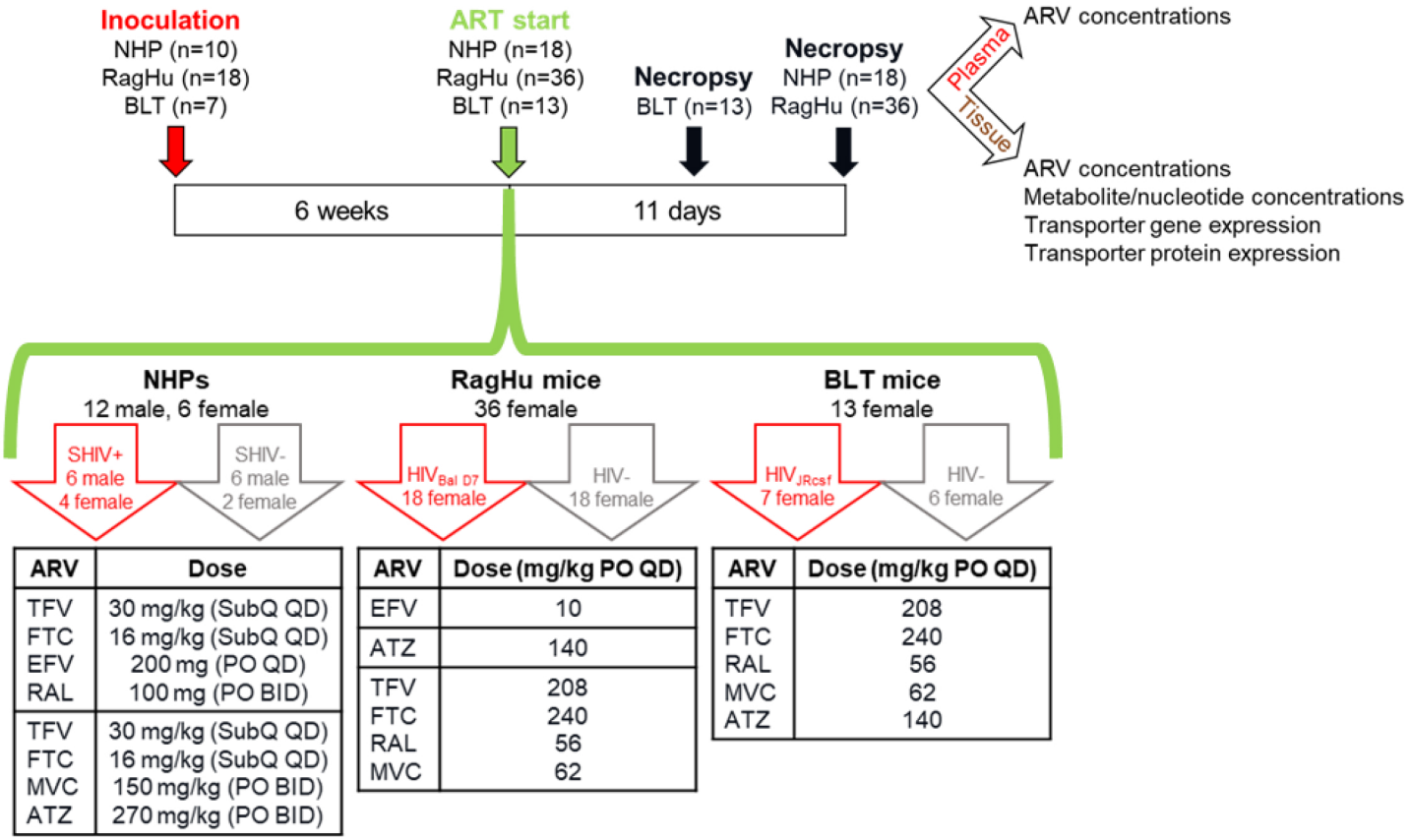

ARV	Dose
TFV FTC EFV RAL	30 mg/kg (SubQ QD) 16 mg/kg (SubQ QD) 200 mg (PO QD) 100 mg (PO BID)
TFV FTC MVC ATZ	30 mg/kg (SubQ QD) 16 mg/kg (SubQ QD) 150 mg/kg (PO BID) 270 mg/kg (PO BID)

ARV	Dose (mg/kg PO QD)
EFV	10
ATZ	140
TFV FTC RAL MVC	208 240 56 62

ARV	Dose (mg/kg PO QD)
TFV FTC RAL MVC ATZ	208 240 56 62 140

Supplementary Figure 1: Infection, dosing, and sampling scheme for animal studies.

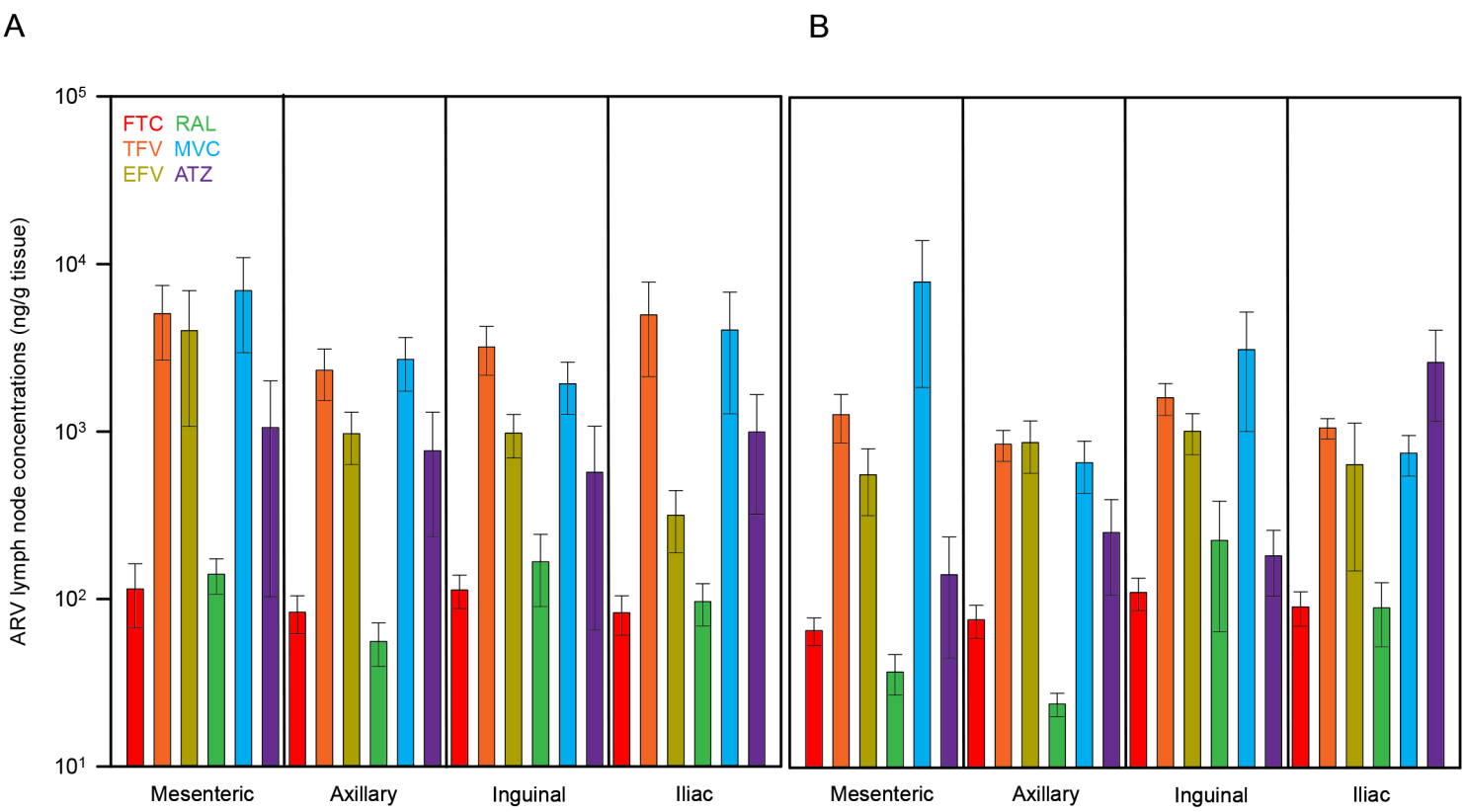

Supplementary Figure 2: ARV concentrations in mesenteric, axillary, inguinal, and iliac lymph nodes collected from (A) SHIV- and (B) SHIV+ NHPs. Bars are mean, and error bars are standard error. Lymph node differences were analyzed using Kruskal-Wallis One-Way ANOVA with Dunn's Method correction for multiple comparisons.

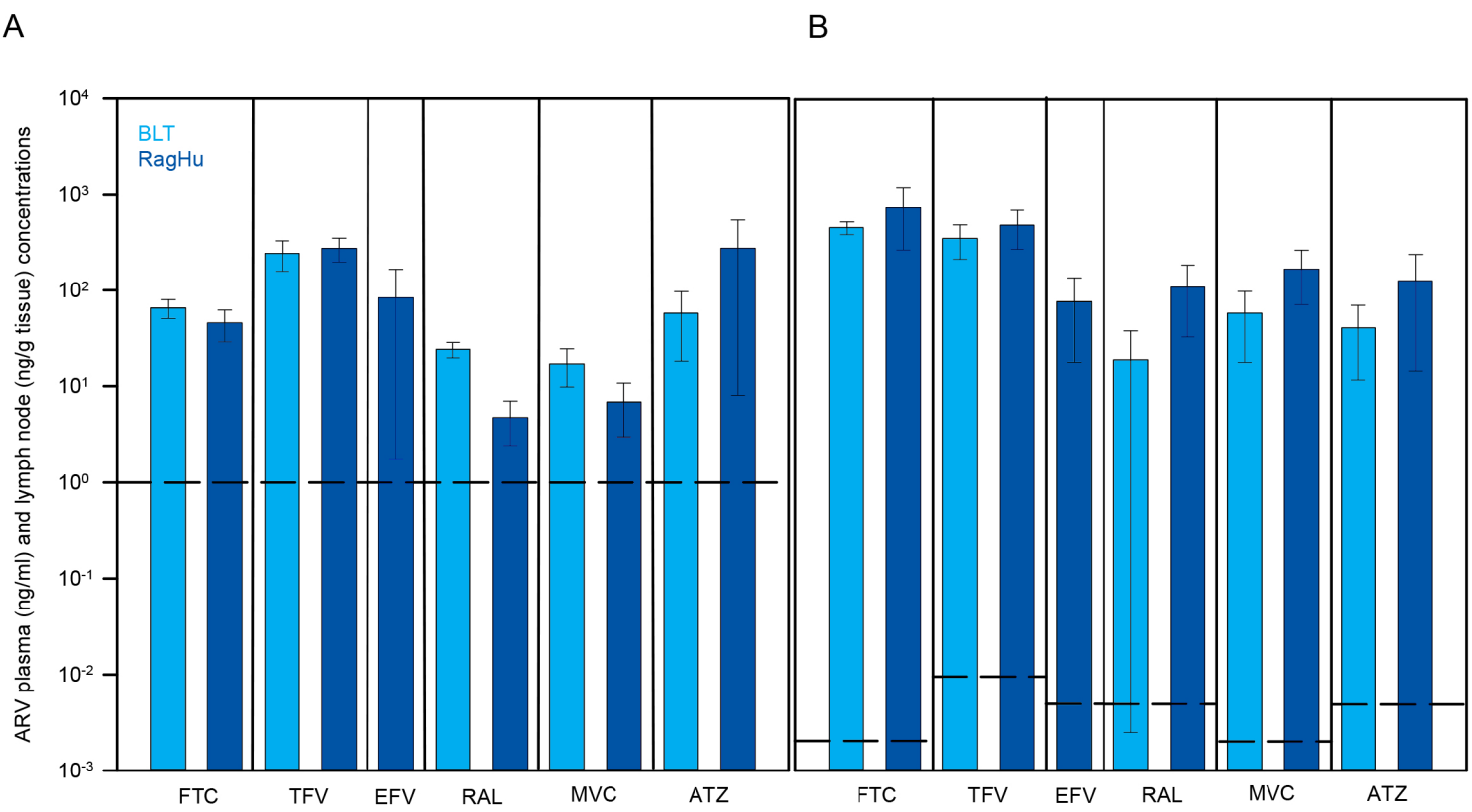

Supplementary Figure 3: ARV plasma (A) and lymph node (B) concentrations in BLT and RagHu humanized mice. Bars are mean, and error bars are standard error. Dashed lines indicate LLOQs. Between-species differences were analyzed using Kruskal-Wallis One-Way ANOVA with Dunn's Method correction for multiple comparisons.